

BEAM TRANSPORT WITH MAGNETIC SOLENOIDS AND PLASMA LENSES

Robert J. Noble
*Fermi National Accelerator Laboratory**
Batavia, Illinois 60510

Abstract

We examine the behavior of axisymmetric space-charge dominated beams in transport lines using numerical simulation. A typical transport line consisting of two axisymmetric linear lenses used to match a continuous beam from an ion source to a radio frequency quadrupole (RFQ) is considered. We compare the beam evolution when both lenses are magnetic solenoids or Gabor plasma lenses for beams with different initial density profiles. Emittance oscillations due to nonlinear space-charge forces are reduced by the action of plasma lenses in which space-charge fields are shielded, but beam mismatch at the RFQ entrance can be significant for both types of lens.

Introduction

The recognition by Lapostolle¹ that changes in space-charge field energy could be related to changes in rms emittance has motivated several efforts to understand and control the evolution of emittance in space-charge dominated beams. For these beams the space-charge term is much larger than the emittance term in the rms envelope equation (for a continuous, unaccelerated beam)

$$d^2R/dz^2 + k^2R - \varepsilon^2/R^3 - K/2R = 0 \quad (1)$$

where $R = \langle r^2 \rangle^{1/2}$ is the rms beam radius, k is the focusing channel wavenumber, $\varepsilon = (\langle r^2 \rangle \langle v^2 \rangle - \langle \bar{r} \cdot \bar{v} \rangle^2)^{1/2}$ is the rms emittance,² $\bar{v} = d\bar{r}/dz$, and K is the generalized beam perveance.³ If we define the characteristic space-charge wavenumber as $k_s = K^{1/2}/\sqrt{2}R$, then the condition for a space-charge dominated beam is $\varepsilon/k_s R^2 \ll 1$.

More recently the numerical simulations of Wangler et al.⁴ have revealed an unexplained, explosive emittance growth in one-quarter of a plasma period for beams in a continuous, linear focusing channel. This growth is followed by damped oscillations at the plasma frequency as the beam density profile oscillates between peaked and hollow distributions.

Despite such unexplained results, the physical picture of rms emittance growth has long been understood. It was recognized that linear space-charge forces arising from a uniform beam profile would not produce rms emittance growth.^{1,5} Nonuniform profiles however result in nonlinear forces, and particle oscillation frequencies then depend on amplitude. The phase space ellipse is distorted into the classic 'S' shape as it rotates.³ This filamentation of the beam phase space changes the rms emittance (dilution), although the actual phase space area is unchanged in the absence of collisions.

Progress in the analytic understanding of emittance growth was made by Anderson,⁶ who used the fact that the internal motion of a space-charge dominated beam is approximately that of laminar flow in a cold beam ($\varepsilon/k_s R^2 \rightarrow 0$) in order to calculate emittance evolution. He showed that the explosive emittance growth observed by Wangler et al.⁴ for a matched beam in a focusing channel is given by $\Delta\varepsilon^2 = (U/2)k_s^2 R^4$, where $U = \int_0^b r dr (E_s/Ne)^2 = (1 + 4 \ln b/\sqrt{2}R)$ is the normalized space-charge field energy of the initial beam, E_s is the initial space-charge field, and the radius b is large enough to include all of the beam. For a general beam profile $U > 0$, and for a uniform profile $U = 0$.

*Operated by the Universities Research Association under contract with the U. S. Department of Energy

Transport Line Simulation

The injection of an ion beam into a drift-tube linac can be easily accomplished with a radio frequency quadrupole (RFQ) which focuses, bunches and accelerates a beam from tens of keV to a few MeV in energy. An RFQ generally requires a narrow, converging axisymmetric beam at its entrance, and lenses are used to "match" the phase space ellipse of the source beam to the RFQ acceptance. The parameters $\alpha = -\langle \bar{r} \cdot \bar{v} \rangle/\varepsilon$ and $\beta = \langle r^2 \rangle/\varepsilon$ are commonly used to specify the beam envelope slope and width, respectively. Envelope integration programs such as TRACE⁷ aid in the design of a beam transport line that will produce a specific α and β at an RFQ entrance. These programs assume that the beam density profile is uniform, and the rms emittance is constant.

To investigate the effect of emittance oscillations on beam matching, a special particle-in-cell (PIC) code was written in FORTRAN. The program uses macroparticles to simulate the internal dynamics of a continuous, axisymmetric beam in a transport line consisting of an arbitrary combination of drift spaces and linear lenses. The beam propagates in the $+z$ direction at a constant velocity in the paraxial approximation. Only transverse space-charge fields and external focusing fields act on macroparticles ($\partial E_{sz}/\partial z \ll 4\pi\rho$, where ρ is the charge density).

An initial beam phase space distribution specified at $z = 0$ is expected to evolve as a function of z under the action of space-charge and external fields. We normalize transverse distances by the initial rms beam radius R_o and the longitudinal distance by the initial space-charge wavenumber $k_{so} = K^{1/2}/\sqrt{2}R_o$. The single-particle dynamics for the simulation can then be described in terms of the dimensionless radial position \bar{r}/R_o , length $k_{so}z$ and velocity (divergence) $d(\bar{r}/R_o)/d(k_{so}z)$ independent of the actual beam size or perveance. Typically 6000 macroparticles are randomly assigned to a radial grid of 300 mesh points according to specified distributions in position and divergence.

At each longitudinal step of the simulation ($\Delta k_{so}z \ll 1$), a standard "leapfrog" algorithm is used to move particles: (1) charge is assigned to mesh points by interpolation according to the position of particles at the last step, (2) space-charge fields are calculated at each mesh point using Gauss's law, (3) the change in particle velocity is calculated by interpolation of the fields at the particle position, and (4) the change in position is found using the new velocity. Because a transported beam oscillates radially, the computational grid is expanded or contracted according to the position of the beam edge at the end of each step in order to maintain resolution.

Magnetic Solenoids and Plasma Lenses

Two degrees of freedom are needed in a transport line to match a round beam's α and β to the RFQ acceptance. In a typical transport line the lens and drift lengths are not easily adjustable after installation, and a minimum of two lenses is required. We will compare the beam evolution through the transport line shown in Fig. 1 when both lenses are magnetic solenoids or Gabor plasma lenses.⁸ An ideal Gabor lens supports a plasma, a radial electric field and an axial magnetic field in equilibrium. The plasma shields the space-charge fields of the beam, and the electric field provides radial focusing. Beam-plasma scattering has a negligible effect on emittance in a typical Gabor lens, and we do not include it in our simulations.

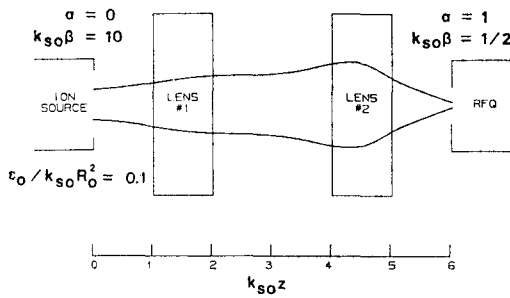


Figure 1: Double-lens transport line showing the evolution of the rms beam envelope calculated from Eqn. (1).

The lens positions and lengths shown in Fig. 1 were arbitrarily chosen symmetrically between the ion source exit and the RFQ entrance. Dimensionless parameters are used to describe the transport line in order to illustrate fundamental scalings independent of beam size and perveance. The beam envelope was obtained by integrating Eqn. (1) starting from a waist with a constant emittance $\epsilon_o/k_{so}R_o^2 = 0.1$. The envelope is essentially the same for magnetic or plasma lenses, although the lens strengths (wavenumbers) are different for the same match:

$$\text{Magnetic: } k_1/k_{so} = 0.953, k_2/k_{so} = 1.167 \quad (2)$$

$$\text{Plasma: } k_1/k_{so} = 0.770, k_2/k_{so} = 1.099. \quad (3)$$

As an example the initial space-charge wavenumber of a beam from a typical proton or H^- source producing several tens of mA current at a few tens of keV energy might be $k_{so} = 0.1 \text{ cm}^{-1}$ with initial mean square beam radius $R_o^2 = 0.1 \text{ cm}^2$. The source rms emittance in Fig. 1 would be $\epsilon_o = 1 \text{ cm mrad}$, with $\beta_{source} = 100 \text{ cm}$ and $\beta_{RFQ} = 5 \text{ cm}$. The transport line length would be 60 cm.

To illustrate the effects of different amounts of space-charge field energy on beam mismatch, we present simulation results from our PIC code for the evolution of initially parabolic ($\rho \sim 1 - (r/a)^2$, $U = 0.0224$) and Gaussian ($\rho \sim \exp(-r^2/\sigma^2)$, $U = 0.154$) beam density profiles. The results are not very sensitive to the initial divergence distribution. A Gaussian divergence distribution was used in these simulations with the initial rms emittance being $\epsilon_o/k_{so}R_o^2 = 0.1$. Gaussian distributions are truncated at two and a half times their rms size.

The emittance oscillations through the transport line containing magnetic (M) and plasma (P) lenses are compared in Fig. 2. The shielding of space-charge fields in the plasma lens is evident from the constant emittance segments on the curves labeled 'P'. For either type of lens, the beam profiles become nearly uniform in the first lens and then hollow in the intermediate drift space. Here some rms emittance is converted back into space-charge potential energy. The beam returns to a uniform profile after the second lens. In the final focus where the RFQ entrance would be, the emittance decreases rapidly, and the beam becomes sharply peaked with a diffuse halo. The halo contains approximately ten percent of the beam with ninety percent of the focused beam being within one and a half rms radii.

Figures 3 and 4 show the evolution of α and $k_{so}\beta$, respectively, in a transport line containing two magnetic lenses (Eqn. (2)) and correspond to the emittance curves labeled 'M' in Fig. 2. The final focus region near $k_{so}z = 6$ is magnified in Figs. 3b and 4b to show the mismatch at the RFQ entrance. The mismatch in α and $k_{so}\beta$ is a combination of emittance growth and differences in rms beam radii and divergences. At $k_{so}z = 6$ the rms beam radius of the initially parabolic beam is a few percent greater than the envelope prediction (Fig. 1) while that of the Gaussian is 40 percent greater. This is partly due to the beam halos which for the parabolic beam extends to about two rms beam radii and for the Gaussian beam to about five rms radii.

Figure 2 indicates that the plasma lenses reduce the emittance oscillations which are so pronounced in the magnetic transport line. However we find that the resulting mismatch in α and $k_{so}\beta$ at the RFQ entrance is not dramatically improved. Figures 5 and 6 show the evolution of α and $k_{so}\beta$, respectively, in a transport line containing

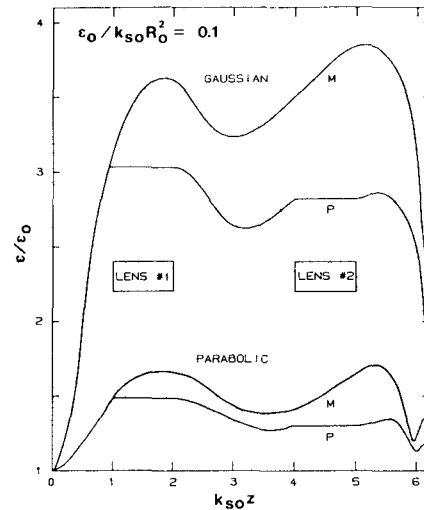


Figure 2: Emittance oscillations for initially parabolic and Gaussian beams in a double-lens transport line when both lenses are either the magnetic (M) or plasma (P) type.

two plasma lenses (Eqn. (3)) and correspond to the emittance curves labeled 'P' in Fig. 2. Comparison with Figs. 3 and 4 indicates only marginal improvement in the beam matching. The plasma lenses do reduce halo formation in the Gaussian beam. At $k_{so}z = 6$ the rms radius is only about 20 percent greater than the envelope prediction, and the halo extends to about four and a half rms radii.

Conclusion

In a double-lens transport line, explosive emittance growth due to nonlinear space-charge forces occurs in the initial drift space, while rapid emittance reduction occurs in the final focus. A shorter initial drift space and a more uniform beam profile are desirable. Because of the large emittance growth in the initial drift, the use of plasma lenses rather than magnetic solenoids did not significantly reduce mismatch in the case studied here. Plasma lenses would be advantageous if the initial drift space was shorter although this may be difficult to achieve in actual transport lines.

References

1. P.M. Lapostolle, *IEEE Trans. Nucl. Sci.* **18**, 1101 (1971).
2. This is the rms emittance in the absence of a uniform axial magnetic field and is understood to contain a compensating term for the Larmor rotation when the beam enters such a field to maintain its invariance, as explained by R.K. Cooper, *Particle Accelerators* **7**, 41 (1975).
3. J.D. Lawson, *Adv. Electronics and Electron Phys., Suppl.* **13C**, 1 (1980). The generalized perveance $K = 2Nr_c/\beta_r^2\gamma_r^3$, where N is the number of beam particles per unit length, r_c is the classical particle radius, and β_r and γ_r are the usual relativistic quantities. The perveance is essentially the ratio of a particle's space-charge potential energy at the beam edge and longitudinal kinetic energy.
4. T.P. Wangler, K.R. Crandall, R.S. Mills and M. Reiser, *IEEE Trans. Nucl. Sci.* **32**, 2196 (1985).
5. F.J. Sacherer, *IEEE Trans. Nucl. Sci.* **18**, 1055 (1971).
6. O.A. Anderson, *Particle Accelerators* **21**, 197 (1987).
7. K.R. Crandall and D.P. Rusthoy, *Documentation for TRACE: An Interactive Beam-Transport Code*, Los Alamos Report LA-10235-MS (Jan. 1985).
8. R.M. Mobley, G. Gammel and A.W. Maschke, *IEEE Trans. Nucl. Sci.* **26**, 3112 (1979).

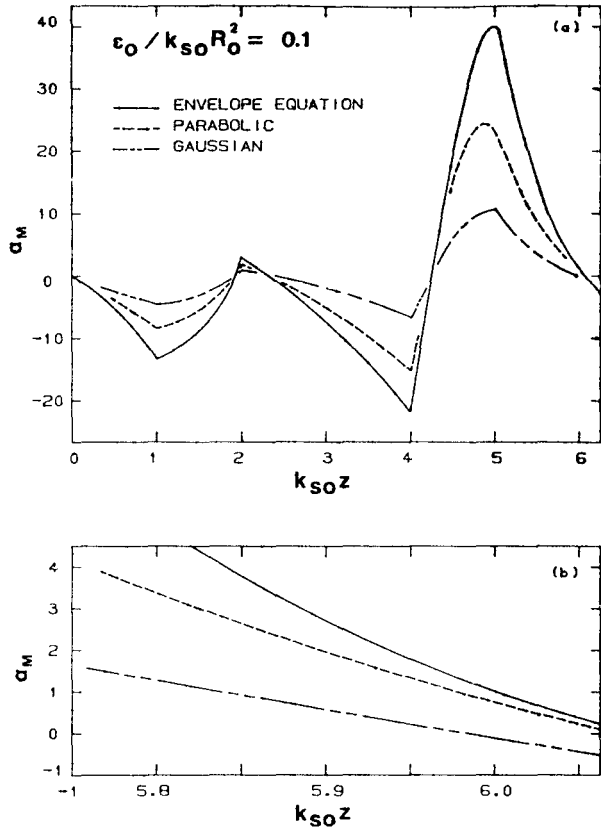


Figure 3: Evolution of α (a) through the transport line containing two magnetic lenses and (b) in the final focus region near $k_{so}z = 6$.

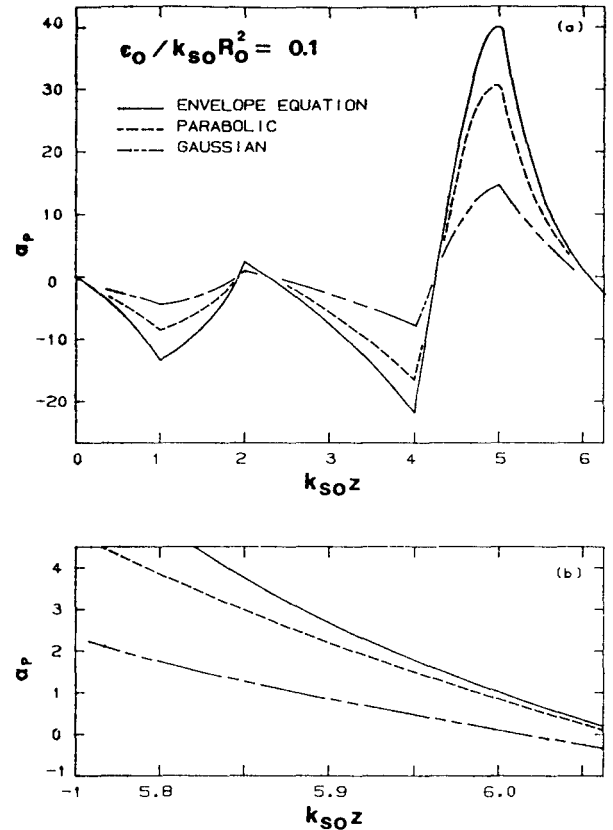


Figure 5: Evolution of α (a) through the transport line containing two plasma lenses and (b) in the final focus region near $k_{so}z = 6$.

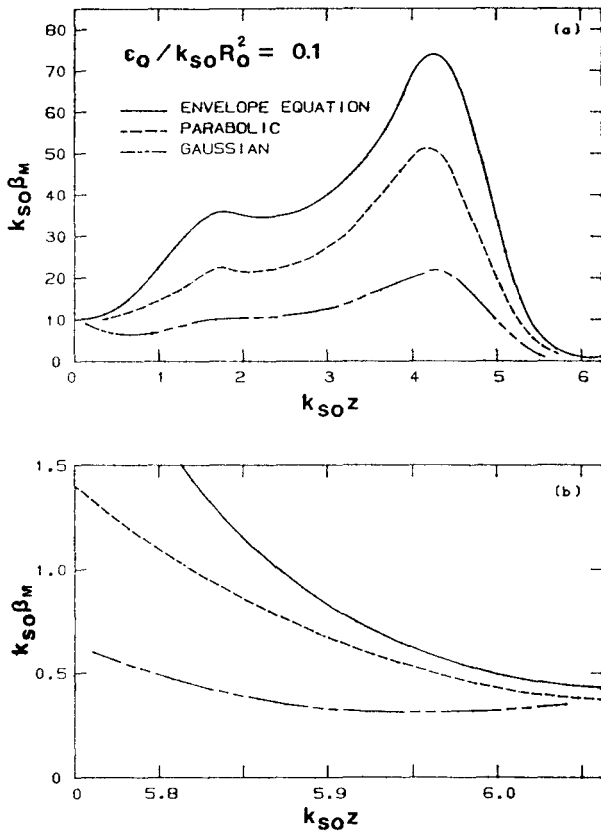


Figure 4: Evolution of $k_{so}\beta$ (a) through the transport line containing two magnetic lenses and (b) in the final focus region near $k_{so}z = 6$.

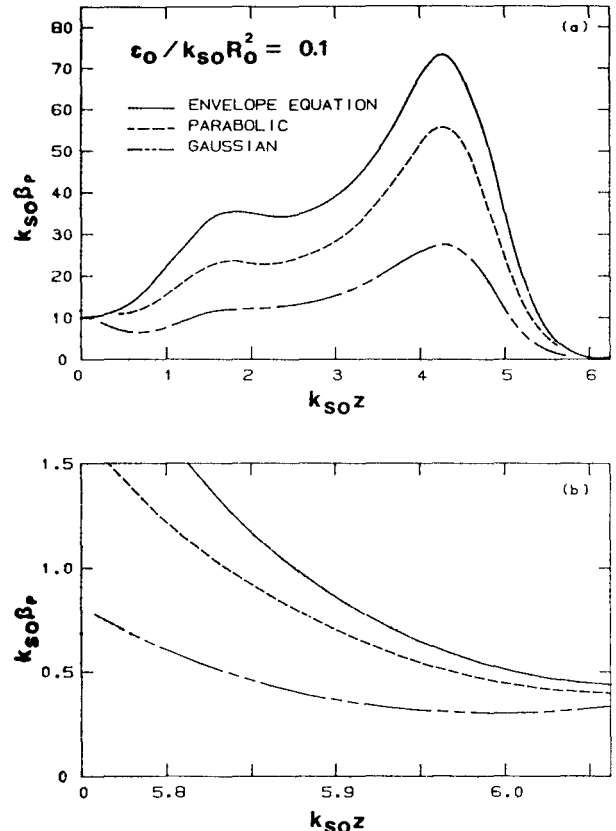


Figure 6: Evolution of $k_{so}\beta$ (a) through the transport line containing two plasma lenses and (b) in the final focus region near $k_{so}z = 6$.